

Article

# Experimental Evaluation of a Spectral Index to Characterize Temporal Variations in the Direct Normal Irradiance Spectrum

Gustavo Nofuentes <sup>1,2,\*</sup>, Christian A. Gueymard <sup>3</sup>, José A. Caballero <sup>4</sup>, Guilherme Marques-Neves <sup>5,6</sup> and Jorge Aguilera <sup>1</sup>

- <sup>1</sup> IDEA Research Group, University of Jaén, Campus de Las Lagunillas, 23071-Jaén, Spain; aguilera@ujaen.es  
<sup>2</sup> Center for Advanced Studies in Earth Science, Energy and Environment (CEACTEMA), University of Jaén, Campus Las Lagunillas, 23071 Jaén, Spain  
<sup>3</sup> Solar Consulting Services, Colebrook, NH 03576, USA; chris@solarconsultingservices.com  
<sup>4</sup> PVhardware Solutions S.L. Polígono Industrial Castilla, Vial I, 13. 46380 Cheste, Spain; chipi.c19@gmail.com  
<sup>5</sup> GDF Research Group, Brazilian National Institute for Space Research, Av. Dos Astronautas, 1758 São José dos Campos, Brazil; gmneves@gmail.com  
<sup>6</sup> Labren Research Group, Brazilian National Institute for Space Research, Av. Dos Astronautas, 1758 São José dos Campos, Brazil  
\* Correspondence: gnofuen@ujaen.es

**Featured Application:** The conclusions of this work may prove highly useful in developing easier models to capture the spectral impact on CPV devices.



**Citation:** Nofuentes, G.; Gueymard, C.A.; Caballero, J.A.; Marques-Neves, G.; Aguilera, J. Experimental Evaluation of a Spectral Index to Characterize Temporal Variations in the Direct Normal Irradiance Spectrum. *Appl. Sci.* **2021**, *11*, 897. <https://doi.org/10.3390/app11030897>

Academic Editor:  
Alejandro Pérez-Rodríguez  
Received: 23 December 2020  
Accepted: 18 January 2021  
Published: 20 January 2021

**Publisher's Note:** MDPI stays neutral with regard to jurisdictional claims in published maps and institutional affiliations.



**Copyright:** © 2021 by the authors. Licensee MDPI, Basel, Switzerland. This article is an open access article distributed under the terms and conditions of the Creative Commons Attribution (CC BY) license (<https://creativecommons.org/licenses/by/4.0/>).

**Abstract:** A simple index is desirable to assess the effects on both flat-plate and concentrating photovoltaics of natural changes in the solar spectrum. Some studies have suggested that the relationship between the Average Photon Energy (APE) and the shape of individual global tilted irradiance, global horizontal irradiance, or direct normal irradiance (DNI) spectra is bijective and can therefore be used as a single number to unequivocally replace a complete spectral distribution. This paper reevaluates these studies with a modified methodology to assess whether a one-to-one relationship really exists between APE and spectral DNI. A 12-month dataset collected in Jaén (Spain) using a sun-tracking spectroradiometer provides the necessary spectral DNI data between 350 and 1050 nm. After quality control and filtering, 78,772 valid spectra were analyzed. The methodology is based on a statistical analysis of the spectral distributions binned in 0.02-eV APE intervals, from 1.74 to 1.90 eV. For each interval, both the standard deviation and coefficient of variation (CV) are determined across all 50-nm bands into which the 350–1050-nm waveband is divided. CV stays below 3.5% within the 450–900-nm interval but rises up to 13% outside of it. It is concluded that APE may be approximately assumed to uniquely characterize the DNI spectrum distribution for Jaén (and presumably for locations with similar climates) only over the limited 450–900-nm waveband.

**Keywords:** spectral irradiance; direct solar spectrum; spectroradiometer; average photon energy; effective wavelength

## 1. Introduction

The accurate estimation of both the expected and predicted electricity yields of photovoltaic (PV) systems is normally carried out by following a standard procedure [1]. This step is crucial to ascertain the production of electricity that such systems may deliver, thus enabling both the bankability of PV projects [2] and the quality assurance for PV plants [3], among other desirable outcomes. After the two quantities (incident broadband irradiance and temperature) that have the most impact on power output, the spectral distribution of the irradiance (spectral irradiance, in short) is generally considered the largest influence to natural variations in the output of clean PV devices [4,5]. It is worth noting that conventional flat-plate PV are less sensitive to varying spectral irradiance than Concentrating

Photovoltaics (CPV). Such a higher sensitivity of the latter technology to spectral effects is especially noticeable when concentrated sunlight of 1000 suns or more is used in High Concentrating Photovoltaics (HCPV) [6], where multi-junction solar cells based on series-connected subcells with different bands of absorption are used in conjunction with optical elements [7,8]. The present contribution is mostly related to the latter type of application.

Spectral effects may be quantified using two methods aimed at estimating a spectral mismatch (MM) factor [9]. The first is based on measurements of the outdoor short-circuit current of the PV device under investigation. The second is based on combining its spectral response with spectra recorded with spectroradiometers—although synthetic or modeled spectra may also be used. One hindrance in the first method is that spectral effects might be difficult to isolate the impacts of device temperature, soiling, or degradation and, in the case of flat-plate PV, angular losses. Hence, the second method is often preferred but requires knowledge of (i) the actual spectrum under the atmospheric conditions at any specific moment (in the case of outdoor exposure) and (ii) the actual spectral response of the PV device under test. The procedure also implies numerical integrations in a 2D domain (wavelength and time). This can become cumbersome if this needs to be repeated at high frequency and can be inexact if the spectral response of the PV device is not known precisely, which is often the case.

To overcome the above difficulties, a simplifying approach—recourse to 1D (time only) spectral indexes that would be independent of the cell's spectral response—has been proposed in the literature. Indeed, such kinds of indexes are often preferred to the integrated useful fraction [10], the spectrally weighted ratio [11], the spectrally corrected global irradiance [12], or other metrics used in non-concentrating PV that depend on the specific device under scrutiny. The same preference holds for some other PV device-dependent indexes used in CPV characterization, such as the Z-parameter [13], the spectrally corrected direct normal irradiance [14], etc. A comprehensive review of spectral indexes has been recently presented [8].

In view of the above, finding a PV device-independent spectral index that could uniquely characterize individual spectra would be most useful for both PV science and engineering. A review of the literature shows that only two such indexes have been investigated and proposed as possible candidates to meet this requirement: the *blue fraction* (BF) and the *average photon energy* (APE). BF has been introduced to assess the ratio of spectral irradiance integrated below 650 nm to the total irradiance [15], whereas APE is the mean energy of all the photons that impinge on a given surface [16].

Despite some early promising results presented by Louwen et al. [17] and later limited results reported by Paudyal and Imenes [18], the possible one-to-one relationship between BF and spectral irradiance still remains highly unexplored. Indeed, this issue has been scarcely addressed thus far [8,18], therefore justifying further investigation. In contrast, APE is an older and more popular index amongst the PV community. It has been widely used to provide a readily qualitative assessment on whether a specific spectrum is shifted to shorter or longer wavelengths relative to the standard spectrum. Thus, a more in-depth analysis of this parameter, including its physical significance, is provided hereafter.

Minemoto et al. [19] first analyzed the relationship between APE and the spectrum shape of global tilted irradiance (GTI). Their experimental campaign was conducted in Kusatsu City, Japan (latitude 34°58' N) over a period of three years. Spectral irradiance was monitored on a 15.3°-tilted surface facing the equator and led the authors to the conclusion that the relationship between APE and the GTI spectrum was bijective. Their methodology was based on an International Electrotechnical Commission (IEC) standard [20], which states by how much the output of a solar simulator can deviate from the AM1.5G reference spectrum. Their reasoning was basically that, if spectral distributions grouped in very narrow APE intervals have a very small standard deviation (SD) in all considered 50-nm bands, such distributions may be considered equal. A closer insight to that methodology is provided in what follows. Subsequent work assumed this one-to-one relationship between

APE and GTI [21–30], although further investigation at other sites was encouraged to confirm the possible universality of such a relationship.

Norton et al. [31] carried out a statistical analysis very similar to that of Minemoto et al. [19], using measurements of spectral global horizontal irradiance (GHI) collected at two sites with different climates: Ispra, Italy (latitude 45°49' N, longitude 8°36' E) and Golden, CO, USA (latitude 39°45' N, longitude 105°13' W). Measurements were recorded for 16 months at the latter location and over two years at the former, using dissimilar instruments and experimental protocols at each site. Norton and coworkers concluded that the relationship between APE and the GHI spectrum shape was bijective. However, these authors also raised the need for further collection and analysis of spectral irradiance data at other sites because firm conclusions could not be drawn from measurements at only two sites.

In contrast, the relationship between the spectral distribution of GTI and APE was found *not* bijective by Dirnberger et al. [12]. They noted that spectral distributions with the same value of APE might yield different values of MM for the same PV material. Their conclusion was based on the analysis of spectral GTI data collected on a 35°-tilt equator-facing surface over a 3.5-year experimental campaign conducted in Freiburg im Breisgau, Germany (latitude 47°59' N).

A later study presented by Nofuentes et al. [32] applied the same methodology as proposed by Minemoto et al. [19] to two spectral datasets collected on a 30°-tilt equator-facing surface during a two-year experimental campaign conducted in two Spanish cities with nearly the same Mediterranean-Continental climate: Jaén (latitude 37°49' N) and Madrid (latitude 40°24' N). These authors underlined that the coefficient of variation (CV) was more appropriate in evaluating the dispersion around the mean than SD alone. Hence, they postulated that spectral distributions with nearly the same APE value should have a small value of CV across all considered 50-nm bands to be considered equivalent. The results obtained for the two Spanish sites under scrutiny showed that bijectivity between APE and GTI spectrum shape could be assumed only from a pragmatic point of view and only over the 450–900-nm waveband, where CV stays below 3.3%. The reasons why noticeable dispersion occurred below 450 nm or above 900 nm were deeply analyzed from both an instrumental standpoint and atmospheric physics principles.

Tsuji et al. [33] carried out a similar statistical analysis to that of Minemoto et al. [19] with spectral GTI data collected on equator-facing surfaces at three Japanese sites for one or two years: Kusatsu (15.3° tilt, as in the study discussed above [19]), Tsukuba (latitude 36°04' N, 20° tilt), and Miyazaki (latitude 31°49' N, 35° tilt). They concluded that APE uniquely represented the spectral distribution of GTI, even though CV values in excess of 30% were found within the 900–950 nm waveband for the three sites under scrutiny.

The literature reviewed above targets flat-plate PV applications only and thus focuses on the *global* spectrum (on either horizontal or tilted surfaces). The bijectivity between APE and spectral direct normal irradiance (DNI) has not received much attention so far, which is a justification for the present investigation. Apparently, Chantana et al. [34] are the only authors who have explored the APE–DNI relationship experimentally and only at a single site. They applied the same general methodology as Minemoto et al. [19] to spectral DNI measurements collected over a one-year experimental campaign conducted in Kusatsu. Chantana and coworkers concluded that a one-to-one relationship did exist between APE and the DNI spectral shape. Unfortunately, they did not analyze the variation of CV across all the studied 10-nm wavebands. It is worth mentioning, though, that a previous theoretical study presented by Gueymard [35] and based on simulations of the cloudless direct spectrum by means of the Simple Model of the Atmospheric Radiative Transfer of Sunshine (SMARTS) I [36] had disproved the bijectivity between APE and the DNI spectral shape. That study showed that different combinations of air mass (AM), aerosol optical depth (AOD), and precipitable water (PW) could result in significantly different DNI spectral distributions with however the same resulting APE value.

The present work aims at exploring whether the APE uniquely characterizes the varying DNI spectrum—at least in practical terms—from an experimental standpoint. In view of the above literature review, this study is the second known attempt to elucidate such an issue by analyzing measured DNI spectra. The present 12-month experimental study is based on spectroradiometric measurements at Jaén, Spain. The general methodology of Nofuentes et al. [32] is followed to perform an appropriate statistical analysis of the spectral data.

## 2. Materials and Methods

### 2.1. Experimental Setup

The experimental campaign was conducted at the University of Jaén (Spain, with a Mediterranean-Continental climate), a small-size city (113,000 inhabitants) where periodic Saharan dust episodes occur in summer, together with high levels of olive-tree pollen during May. A comprehensive description of this site in atmospheric terms was carried out in a previous work [32].

The empirical data used in this paper was collected at the outdoor research facilities located on the flat roof of one of the buildings of the High Technical School of the Engineering and Technology campus, located within the city. These facilities were described in detail in previous studies [37,38].

The direct spectrum was measured by an EKO<sup>TM</sup> MS700 spectroradiometer equipped with a collimator tube and fixed to a two-axis BSQ<sup>TM</sup> D1506 solar tracker for concentrating PV applications, as shown in Figure 1. The collimator tube was made of black PVC and was devised according to the values of the slope angle ( $1^\circ$ ) and aperture angle ( $5^\circ$ ) specified in the MS700 spectroradiometer datasheet. This experimental setup has been successfully used in earlier work [39].

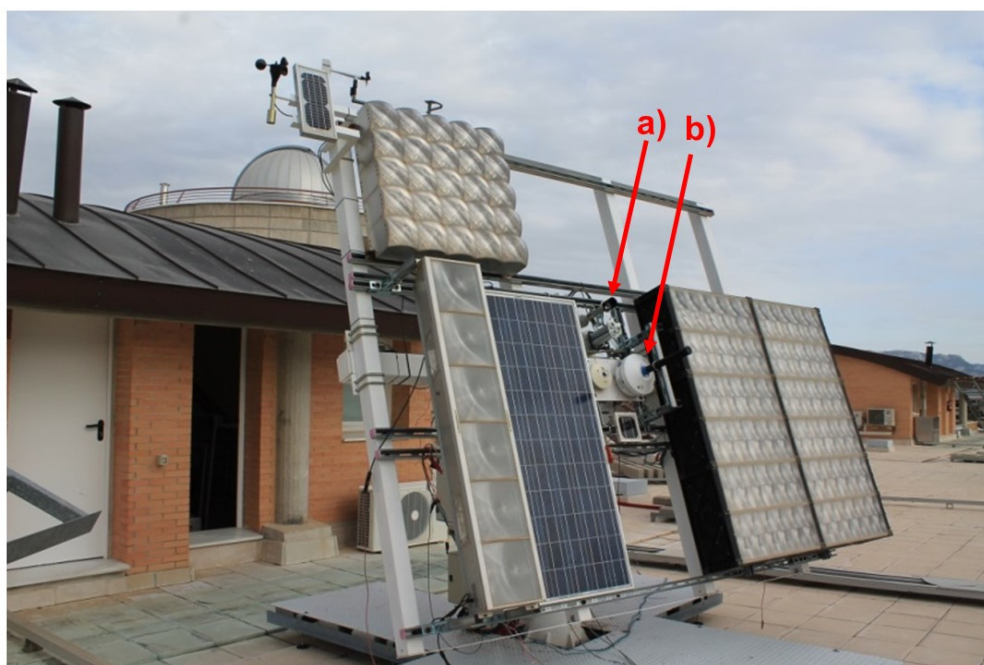


**Figure 1.** Pyrheliometer (a) and spectroradiometer with collimator tube (b) used in this work.

The specifications of the above instrumentation include a 10-nm spectral resolution, a wavelength interval of  $\approx 3.3$  nm between 350 and 1050 nm, and a temperature dependency of  $\pm 1\%$  between  $-20$  and  $+50$  °C. The 12-month monitoring period extended from March 2013 to February 2014 at different time intervals. Observations were normally done every 20 s, but the interval had to be relaxed to 5 min during a few periods; this did not influence the results, as discussed in Section 2. The instruments were calibrated by the manufacturer

just before the experimental campaign and after it, in October 2014, with no significant change in sensitivity. Additionally, the broadband DNI was measured with a first-class Kipp & Zonen CHP 1 pyrhelimeter. Spectral instances recorded while the broadband DNI was below  $50 \text{ W}\cdot\text{m}^{-2}$  were excluded to avoid the noise introduced by a low signal. Neglecting these measured spectra does not affect the calculations to be presented in what follows because the annual DNI fraction collected below this threshold only accounts for  $\approx 1\%$  in Jaén [38]. After filtering of the data, 78,772 valid DNI spectra were available for further analysis.

As discussed earlier, the possible bijectivity between APE and spectral DNI for a given site was apparently investigated in only one study so far [34]. Thus, it is worth mentioning that the same spectroradiometer brand and model that was used in their work is also used here, thus making any comparison of results impervious to experimental differences. Their data filtering and its subsequent processing do not differ substantially from that presented in this paper either, except in a few aspects that will be described hereafter.

## 2.2. Average Photon Energy

Originally proposed by Jardine et al. [16] to qualitatively assess the shape of the spectral irradiance, APE is the average energy of the photons over a specific spectrum distribution. It may be expressed as follows:

$$\text{APE} = \frac{\int_a^b E(\lambda) d\lambda}{\int_a^b \Phi_{\text{ph}}(\lambda) d\lambda} \quad (1)$$

where  $E(\lambda)$  in  $\text{W}\cdot\text{m}^{-2}\cdot\text{nm}^{-1}$  is the spectral irradiance,  $\Phi_{\text{ph}}(\lambda)$  in  $\text{m}^{-2}\cdot\text{nm}^{-1}\cdot\text{s}^{-1}$  is the spectral photon flux density, and  $a$  in nm and  $b$  in nm are the lower and upper limits, respectively, of the considered waveband of the solar spectrum. Solar spectra rich in photons with shorter wavelengths yield higher values of APE, whereas solar spectra rich in photons with longer wavelengths yield lower values of APE.

An equivalent definition was proposed later [35]:

$$\text{APE} = hc(kq\lambda_{\text{eff}})^{-1}, \quad (2)$$

where

$$\lambda_{\text{eff}} = \frac{\int_a^b \lambda E(\lambda) d\lambda}{\int_a^b E(\lambda) d\lambda} \quad (3)$$

and where  $\lambda_{\text{eff}}$  is the “effective wavelength” in nm,  $h$  is the Planck constant,  $c$  is the speed of light in vacuum,  $q$  is the electronic charge, and  $k$  is a constant to reconcile units, equal here to  $1 \times 10^{-9}$  for  $\lambda_{\text{eff}}$  expressed in nm. By using Equation (2), possible variations in APE are intuitively linked to varying incident irradiance spectral balances. Thus, blue-biased spectra are conducive to shorter effective wavelengths, which in turn lead to higher values of APE. Conversely, red-biased spectra—conducive to larger values of  $\lambda_{\text{eff}}$ —lead to lower values of APE.

Obviously, the value of APE also depends on the considered spectral range. In this sense, the 350–1050 nm waveband (typically sensed by the silicon-based detectors used in many commercial spectroradiometers) has been used to calculate APE in many previous studies [16,19,32,34,40–44]. For that specific waveband, the values of APE for the AM1.5G and AM1.5D reference spectra equal 1.878 and 1.846 eV, respectively. The corresponding effective wavelengths are 662.6 and 671.7 nm, respectively. The slight red shift in the DNI spectrum compared to the GTI spectrum results from the latter’s inclusion of diffuse irradiance, which is rich in blue wavelengths.

### 2.3. Methodology

As commented on in Section 1, the methodology initially proposed by Minemoto et al. [19] and followed by Chantana et al. [34], is applied as closely as possible in this investigation to assess whether a given APE value is *uniquely* linked to a specific DNI spectrum shape. However, as discussed in Section 1, such a methodology is improved here by adding a detailed analysis of variance, as argued by Nofuentes et al. [32]. In that study, the coefficient of variation (CV)—defined as the percentage ratio of the standard deviation (SD) to the mean—was shown to provide a better insight into the scatter around the mean than SD alone.

Based on previous experience, the design of the APE analysis procedure used in this work was articulated with the steps described below:

- (1) The trapezoidal rule was used to calculate the broadband DNI between 350 and 1050 nm for each experimental direct spectrum. (That calculated DNI value was obviously smaller than the reading from the pyrheliometer, for which the spectral range was  $\approx 290\text{--}4000$  nm.)
- (2) Equation (1) was used to calculate the APE for each DNI spectrum.
- (3) The wavelength range was divided into fourteen 50-nm bands—from 350 to 1050 nm—for each spectral instance. The fractional contribution of each 50-nm spectral band to the broadband irradiance ( $R_c$ ) calculated in step 1 was obtained.
- (4) All the DNI spectral measurements were grouped into APE intervals of 0.02-eV width. More specifically, eight intervals ranging from 1.74–1.76 eV to 1.88–1.90 eV were considered. Spectral measurements having an APE within  $\pm 0.01$  eV of the central value of each of these intervals were binned inside them.
- (5) For every APE interval and within each 50-nm band, spectral measurements with  $R_c$  values below the 10th percentile or above the 90th percentile were eliminated to minimize the influence of outliers.
- (6) For every APE interval defined in step 4, mean values of  $R_c$  (denoted  $\langle R_c \rangle$ ) were calculated in each 50-nm band. Values of SD and CV were also obtained for each of these bands to determine the dispersion of the values of  $R_c$  around its mean value for every APE interval.

As mentioned in Section 1, it should be kept in mind that the analysis carried out by Chantana et al. [34] considered seventy-one 10-nm spectral bands into which the 350–1050 nm waveband was divided instead of the fourteen 50-nm bands considered here (step 3, above).

### 3. Results and Discussion

The recorded spectral instances that are outside the eight APE intervals stated in step 4 and removed according to step 5 of Section 2.2 account for less than 17% of the whole 12-month experimental database. After filtration, 65,881 spectral instances remained.

It is worth investigating to what extent the local spectral distribution for values of APE close to its standard value (1.846 eV) align with that of the standard spectrum when AM values are close to 1.5. Figure 2 shows the mean percentage contributions of every 50-nm band considered in this work relative to the integrated DNI for measured spectra in which APE and AM are within 1.84–1.86 eV and 1.45–1.55, respectively. The values of  $R_c$  for each of the fourteen bands are shown for the reference spectrum as well. The latter seems to coincide reasonably well with local AM1.5D distributions. The fact that spectral DNI measurements with APE values in the vicinity of 1.85 eV closely resemble the distribution of the reference spectrum is according to expectations and confirms what was already noted by Chantana et al. [34] based on experimental measurements at Kusatsu, Japan. Nevertheless, a careful analysis shows that, despite being apparently small, the SD values obtained at both Jaén and Kusatsu are not negligible when compared to the  $\langle R_c \rangle$  values across the 50-nm band intervals used here—or 10-nm bands for the Japanese site—that lie outside the central wavelength range (450–900 nm). This dispersion of percentage contributions within the 350–450 nm and 900–1050 nm wavebands was also noted in local GTI spectral distributions for APE and AM around 1.88 eV and 1.5, respectively

(corresponding to the AM1.5G spectrum) for Jaén [32]. These two results are mutually consistent because the AM1.5G spectrum is essentially composed of direct irradiance (see, e.g., Figure 10 of [45]).

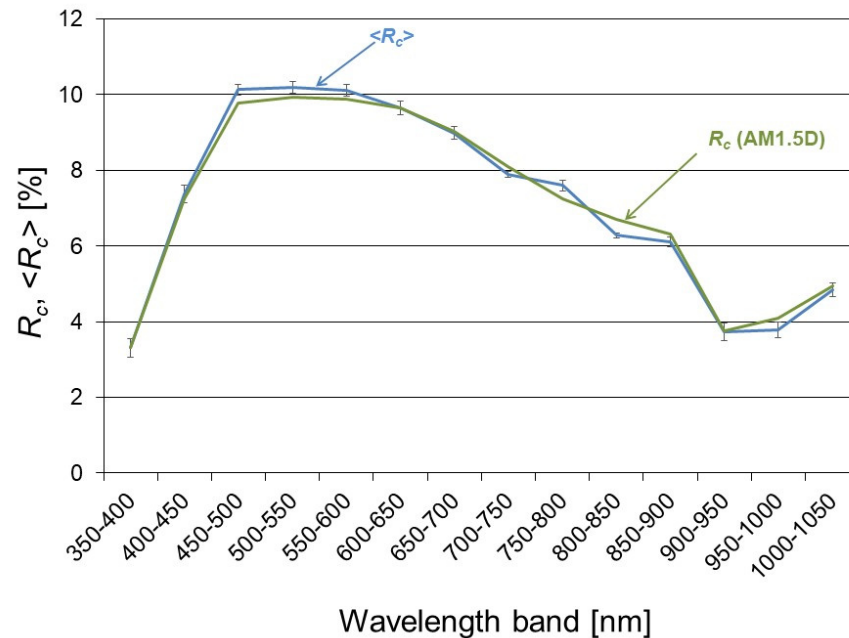


**Figure 2.** Mean percentage contributions to direct normal irradiance (DNI)—integrated from 350 to 1050 nm—across all 50-nm bands for spectral measurements with Average Photon Energy (APE) and air mass (AM) values of  $1.85 \pm 0.01$  eV and  $1.5 \pm 0.05$ , respectively, recorded at Jaén (blue line); error bars indicate the standard deviation (SD) values related to each of these bands. The “reference”  $R_c$  values calculated for each of these bands from the standard AM1.5D spectrum are also shown (green line).

The AM values corresponding to the spectral measurements recorded over the course of the 12-month experimental campaign spread over a large interval, 1.03–16.00; the calculated average AM is 2.19 and, hence, significantly above the standard 1.5 value. In parallel, the broadband DNI values obtained from the pyrheliometer range from 50 to  $1047 \text{ W}\cdot\text{m}^{-2}$  and average  $715 \text{ W}\cdot\text{m}^{-2}$ , far lower than the  $900 \text{ W}\cdot\text{m}^{-2}$  standard value. This could be expected because DNI decreases rapidly when AM increases or when thin clouds partly obscure the sun’s disc.

Figure 3 shows the values of  $\langle R_c \rangle$  for every 50-nm band according to each APE bin into which the spectral measurements have been grouped. Higher values of APE imply shorter values of  $\lambda_{\text{eff}}$  and, thus, higher relative contributions of shorter wavelengths relative to the integrated DNI within 50-nm bands. Conversely, values of  $\langle R_c \rangle$  corresponding to 50-nm bands with longer wavelengths are enhanced as APE decreases (and  $\lambda_{\text{eff}}$  increases). Interestingly, note that  $\langle R_c \rangle$  tends to remain constant in the 600–650-nm spectral band, possibly because it corresponds to the “balance” wavelength for the 350–1050-nm spectrum, close to the effective wavelength of the AM1.5D standard spectrum. It is also worth noting that the results shown in Figure 3 are quite well aligned with those obtained by Chantana et al. [34] in their investigation of the purported one-to-one relationship between APE and the DNI spectrum in Kusatsu (see their Figure 5a).

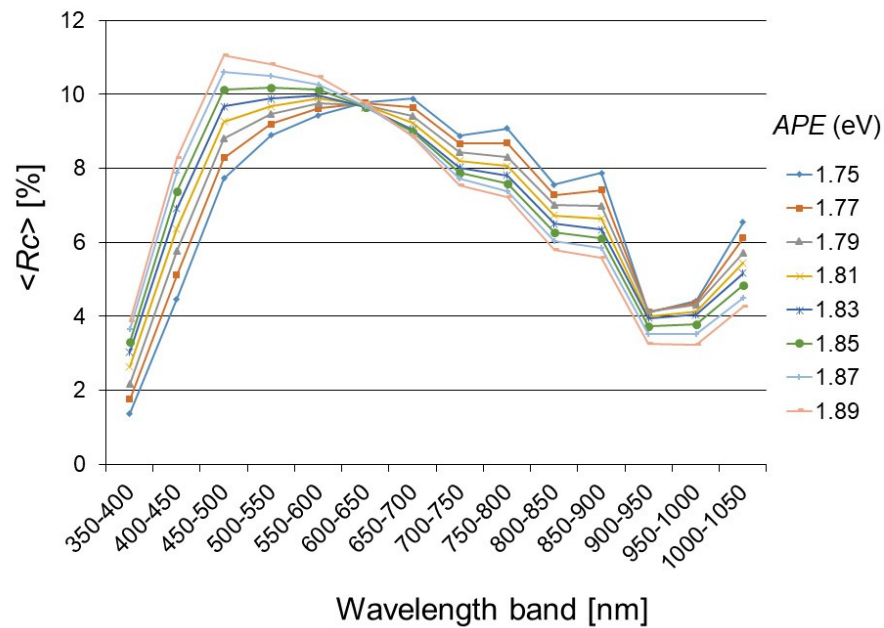


**Figure 3.** Mean values of relative contributions to DNI—integrated from 350 to 1050 nm—across all 50-nm bands for spectral measurements binned in 0.02-eV-width APE intervals over the range 1.75–1.89 eV (central values), using direct irradiance spectra recorded at Jaén.

Moreover, the results depicted in Figure 3 appear to be a good match for those obtained by Minemoto et al. [19] (also for Kusatsu), Norton et al. [31] (for Ispra and Golden, Colorado), Nofuentes et al. [32] (for Jaén and Madrid), and Tsuji et al. [33] for three Japanese cities: Kusatsu, Tsukuba, and Miyazaki. It should be kept in mind, though, that the work presented here is not strictly comparable with these studies, as they were carried out to elucidate the possible bijectivity between APE and either the GTI or GHI spectral distribution.

Table 1 provides details about the distribution of the spectral measurements binned by their corresponding APE interval. For each of these APE intervals, Table 1 also indicates the corresponding effective wavelength, in conjunction with the maximum, minimum, and mean SD values related to the relative contribution to the integrated 350–1050-nm DNI across the fourteen 50-nm bands under scrutiny. Note that only three APE bands ( $1.79 \pm 0.01$  eV,  $1.81 \pm 0.01$  eV, and  $1.83 \pm 0.01$  eV) account for 80% of the spectral instances recorded. Moreover, only less than 1% of the spectral measurements are grouped in bins with APE greater than 1.85 eV, which indicates prevailing red-shifted spectra for the site under investigation. As expected from fundamentals of statistics, the scatter around the mean is larger in APE intervals with fewer samples. In spite of this, the maximum values of SD stay below 0.40%. In comparison, the SD values obtained by Chantana et al. [34] at Kusatsu across all the seventy-one 10-nm bands within the 350–1050 nm spectral range do not exceed 0.20%. Remarkably, SD peaks in the same wavebands (350–400 nm and 900–950 nm) at Kusatsu and Jaén, which deserves scrutiny.

As discussed before [32], SD alone is not enough to suitably assess the dispersion of  $R_c$  around its mean for each APE interval across the 350–1050 nm range. Instead, CV is a more meaningful parameter intended for such purpose.

Figure 4 shows the CV values obtained for each 50-nm band grouping defined above. Within the 450–900-nm waveband, CV stays below  $\approx 3.5\%$  in contrast with the 900–1050-nm waveband, where CV is found to reach much larger values, close to 10%. Higher spikes even occur in the 350–450-nm waveband, where CV reaches up to 13%.

**Table 1.** Maximum, minimum, and mean values of SD of  $R_c$  for every 50-nm band according to their APE interval and corresponding effective wavelength,  $\lambda_{\text{eff}}$ .

Central Value of APE Interval (eV)	$\lambda_{\text{eff}}$ for the Central Value of APE Interval (nm)	SD <sub>max</sub> (%)	SD <sub>min</sub> (%)	SD <sub>med</sub> (%)	Number of Samples	Waveband where SD <sub>max</sub> Occurs (nm)	Waveband where SD <sub>min</sub> Occurs (nm)
1.75	709	0.39	0.09	0.21	4123	900–950	800–850
1.77	701	0.38	0.09	0.20	7195	900–950	800–850
1.79	693	0.36	0.08	0.19	13,962	900–950	800–850
1.81	685	0.26	0.08	0.15	21,116	900–950	800–850
1.83	678	0.21	0.06	0.12	17,727	900–950	800–850
1.85	670	0.25	0.07	0.17	1317	350–400	800–850
1.87	663	0.35	0.07	0.19	338	350–400	800–850
1.89	656	0.31	0.09	0.19	103	350–400	800–850

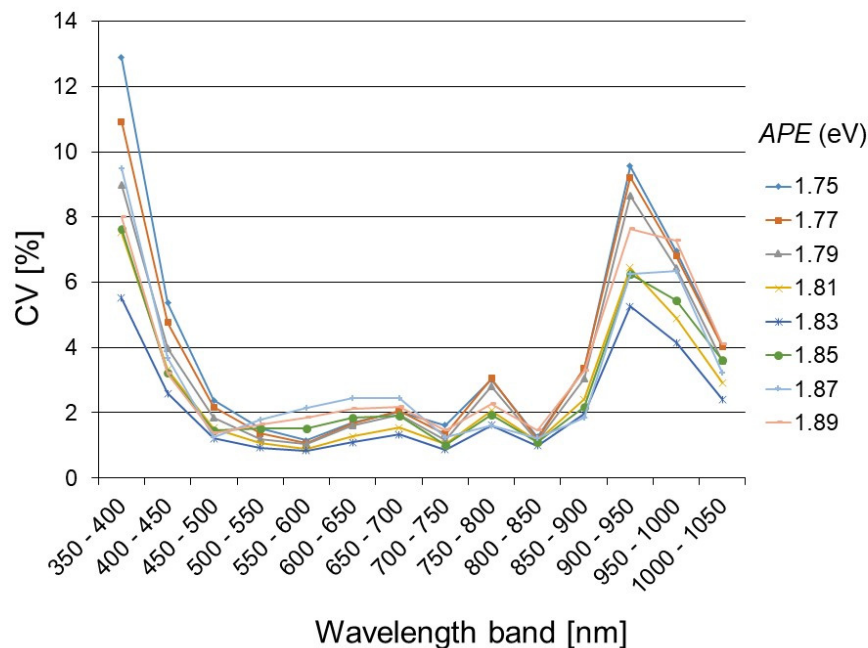


**Figure 4.** Coefficient of variation of  $R_c$  across all 50-nm bands for spectral measurements binned in 0.02-eV width APE intervals over the range 1.75–1.89 eV (central values), using experimental spectral measurements at Jaén.

In practical terms, such results suggest that APE can be assumed to *uniquely* represent the shape of the direct spectrum within the central 450–900-nm wavelength range *only*. Following an identical procedure to that described in Section 2.2, Nofuentes et al. [32] came to the same conclusion for Jaén and Madrid regarding the purported one-to-one relationship between APE and spectral GTI. The present confirmation of the findings in [32] is likely related to the similarity between the GTI and DNI spectra under cloudless conditions, as mentioned above. Interestingly, CV values up to 6% and over 30% within the 350–400 nm and 900–1050 nm wavebands, respectively, were found in Japan [33]. However, despite the fact that such high CV values indicate a large scatter of  $R_c$  around its mean, Tsuji et al. [33] claimed that APE is a unique characteristic of the GTI spectrum distribution. In any case, the results depicted in Figure 4 deserve some further discussion from both the experimental and theoretical standpoints.

The expanded uncertainties ( $U_{95}$ ) for the spectral measurements obtained with the present spectroradiometer used are  $\pm 10.89\%$ ,  $\pm 4.13\%$ , and  $\pm 4.06\%$  for the 350–450 nm, 450–900 nm, and 900–1050 nm wavebands, respectively, according to the certificate of calibration issued by the manufacturer. No significant additional uncertainty resulting from actual outdoor laboratory measurement conditions is likely because the instrument was cleaned each working day. It was, however, not cleaned during a week in March 2013 and another week in August 2013. Given the relative short periods of time during which the instrument remained uncleaned, no significant differences were found between spectral data collected in such periods relative to those gleaned over the course of the entire experimental campaign.

The dispersion noticed for  $R_c$  below 450 nm and the resulting higher values of CV may be explained in part by the higher values of  $U_{95}$  at these shorter wavelengths. As discussed previously [32], however, another contribution is likely related to the substantial daily variance in AOD, which has a large impact on the direct spectrum at short wavelengths [46]. In contrast, the lowest  $U_{95}$  values occur above 900 nm, where CV also peaks. This would seem paradoxical if  $U_{95}$  was the only driver of CV variations along the spectrum, which thus requires scrutiny. As mentioned by Nofuentes et al. [32], it should be borne in mind that the instrument undergoes calibration indoors in a laboratory at a constant ambient temperature (25 °C), thus avoiding the potential impact of large temperature excursions

during sunny days. Those field conditions could influence the reading accuracy in the NIR part of the spectrum much more than at shorter wavelengths [47,48]. This temperature effect should be small here, however, because the detector core of this specific instrument is temperature controlled and has a specified temperature range of  $-10$  to  $50$  °C. A more likely explanation for the high CV in the NIR is that the spectral irradiance is weak there due to water vapor absorption. Therefore, measurements in that band are more vulnerable to the influence of noise, which increases the actual measurement uncertainty. Moreover, water vapor conditions (characterized by PW) are variable on a daily basis over Jaén, which creates strong variance in the 900–950 nm waveband, where water vapor absorption is the strongest relative to the whole 350–1050 nm range.

The results shown in Figure 4 confirm previous theoretical findings obtained by means of synthetic spectra generated by the SMARTS radiation model for various ideal atmospheric conditions [35]. Both modeled and experimental spectra obtained under variable conditions show that AM and AOD influence APE in a way that longer wavelengths are enhanced when they increase (red shift). On the other hand, PW has a more limited but antagonistic effect (blue shift). Hence, different sets of conditions (AM, AOD, and PW) could lead to dissimilar spectral distributions of DNI that would exhibit the same value of APE. As a result, Gueymard [35] concluded that APE was not appropriate to characterize the DNI spectral shape with a single number. The present results tend to confirm that finding.

#### 4. Conclusions

This study investigated whether the average photon energy (APE) uniquely represents the direct normal irradiance (DNI) spectrum over the 350–1050 nm band at Jaén, a Spanish sunny site with Mediterranean-Continental climate. No previous study focusing on the application of APE to the direct spectrum is known except at a Japanese location in a different climate.

The methodology used here is based on a procedure that was previously applied to assess the possible bijectivity between APE and the global tilted irradiance (GTI) spectrum at both Jaén and Madrid. This procedure centers on the analysis of the coefficient of variation (CV) of the relative importance of contributions of 50-nm bands compared to the integrated DNI (from 350 to 1050 nm) of the spectral distributions binned in specific APE intervals.

DNI spectra from 350 to 1050 nm were collected over the course of a 12-month experimental campaign. Over the range 450–900 nm, spectral distributions obtained for an APE of  $\approx 1.85$  eV and air mass (AM) of  $\approx 1.5$  match quite well that of the standard AM1.5D spectrum used as reference in concentrating photovoltaic applications. Nevertheless, some scatter is noticed outside of this central band. Likewise, spectral distributions corresponding to measurements binned in the same APE interval are well aligned within 450–900 nm, where CV remains below  $\approx 3.5\%$ . In contrast, this concordance does not hold outside of that spectral range, considering that CV reaches values of up to  $\approx 10\%$  and  $13\%$  within 350–450 nm and 900–1050 nm, respectively. This significant scatter at shorter wavelengths is only partially ascribed to the measurement uncertainty of the spectroradiometer reported by the manufacturer, which is relatively large below 450 nm. Theoretical considerations reveal that another explanation for the high CV there is related to the temporal variance in aerosol optical depth, which is significant at Jaen, and results in a more or less pronounced red shift in the spectrum. In contrast, the measuring uncertainty is far smaller beyond 900 nm, but steep temperature excursions during the day may influence measurements. Additionally, weak signal levels around the water vapor absorption band (940 nm) are especially vulnerable to noise, thus conducting an increased uncertainty related to the measurements in such band. Temporal variance in atmospheric precipitable water also induces a more or less significant blue shift of the spectrum.

From a theoretical standpoint, the results presented here confirm previous radiative transfer simulations that rejected the APE bijectivity by showing how a single APE value

could be obtained by combining different values of air mass, aerosol optical depth, and precipitable water, thus shaping significantly different DNI spectral distributions.

To summarize, the results presented in this study disprove the currently assumed one-to-one relationship between APE and the spectral DNI within the *whole* 350–1050 nm waveband. Rather, APE may only be assumed to uniquely characterize the DNI spectrum distribution *only* from  $\approx 450$  to 900 nm for Jaén in practical terms. Hence, this limited band is recommended when using APE to model the spectral impact on concentrating PV devices. The present findings confirm those from a previous work that focused rather on the GTI spectrum, which is the reference for flat-plate PV applications. The present conclusion that bijectivity is valid over only a part of the DNI spectrum presumably holds for sites with a similar climate as Jaén, although further verification is needed. Hence, further collection and analysis of spectrally resolved DNI data are desirable at more sites worldwide to better evaluate the impact of local climate, since this type of experimental methodology has been done so far at only two sites in relatively temperate climates, which do not allow drawing general conclusions on a worldwide basis.

**Author Contributions:** Conceptualization, methodology, and writing—review and editing, G.N.; conceptualization, methodology, supervision, and writing—review and editing, C.A.G.; software and data curation, J.A.C.; software, G.M.-N.; funding acquisition, project administration, and supervision, J.A. All authors have read and agreed to the published version of the manuscript.

**Funding:** This research was funded by the Spanish Science and Innovation Ministry (*Ministerio de Ciencia e Innovación de España*) and the ERDF, grant number ENE2009-08302, within the frame of the Project “Analysis and characterization of a concentrated PV system under natural sunlight. Comparison with other PV technologies” (*Análisis y caracterización de un sistema fotovoltaico de concentración a sol real. Comparativa con otras tecnologías fotovoltaicas*). This work was also funded by the Department of Science and Innovation of the Regional Government of Andalucía (*Consejería de Innovación, Ciencia y Empresa de la Junta de Andalucía*), grant number P09-TEP-5045, within the frame of the Project “Analysis and characterization of a concentrated PV system under natural sunlight. Comparison with other PV technologies” (*Análisis y caracterización de un sistema fotovoltaico de concentración a sol real. Comparativa con otras tecnologías fotovoltaicas*).

**Institutional Review Board Statement:** Not applicable.

**Informed Consent Statement:** Not applicable.

**Data Availability Statement:** Not applicable.

**Acknowledgments:** Guilherme Marques-Neves acknowledges the Brazilian National Council for Scientific and Technological Development (CNPq) for granting a scholarship to support his stay at the University of Jaén. The authors greatly acknowledge the technical support of Beatriz García-Domingo and Miguel Torres Ramírez during the experimental campaign.

**Conflicts of Interest:** The authors declare no conflict of interest. The funders had no role in the design of the study; in the collection, analyses, or interpretation of data; in the writing of the manuscript; or in the decision to publish the results.

## Abbreviations

### Terminology

DNI	Direct normal irradiance
GHI	Global horizontal irradiance
GTI	Global tilted irradiance
IEC	International Electrotechnical Commission
PV	Photovoltaic(s)
SMARTS	Simple Model of the Atmospheric Radiative Transfer of Sunshine

**Symbols**

$a$	Lower wavelength limit of an interval of the spectrum (nm)
AM	Air mass
APE	Average photon energy (eV)
AOD	Aerosol optical depth at any wavelength
$b$	Upper wavelength limit of an interval of the spectrum (nm)
BF	Blue fraction
CV	Coefficient of variation (%)
$E(\lambda)$	Spectral Irradiance of the actual solar spectrum ( $W \cdot m^{-2} \cdot nm^{-1}$ )
MM	Spectral mismatch factor
PW	Precipitable water (cm)
$R_c$	Percentage contribution of a spectral band of a recorded spectral (%) measurement to the broadband irradiance
SD	Standard deviation of $R_c$ for every 50-nm band and the same APE interval (%)
$SD_{max}$	Maximum value of standard deviation of $R_c$ for every 50-nm band and the same APE interval (%)
$SD_{mean}$	Average value of standard deviation of $R_c$ for every 50-nm band and the same APE interval (%)
$SD_{min}$	Minimum value of standard deviation of $R_c$ for every 50-nm band and (%) the same APE interval
$U_{95}$	Expanded uncertainty related to spectral measurements (%)
UF	Useful fraction
$\Phi_{ph}(\lambda)$	Spectral Photon Flux Density ( $m^{-2} \cdot nm^{-1} \cdot s^{-1}$ )
$\lambda_{eff}$	Effective wavelength (nm)

**References**

- IEC 61724-1. *Photovoltaic System Performance—Part 1: Monitoring*; International Electrotechnical Commission (IEC): Geneva, Switzerland, 2017.
- Leloux, J.; Lorenzo, E.; García-Domingo, B.; Aguilera, J.; Gueymard, C.A. A Bankable Method of Assessing the Performance of a CPV Plant. *Appl. Energy* **2014**, *118*, 1–11. [[CrossRef](#)]
- De la Parra, I.; Muñoz, M.; Lorenzo, E.; García, M.; Marcos, J.; Martínez-Moreno, F. PV Performance Modelling: A Review in the Light of Quality Assurance for Large PV Plants. *Renew. Sustain. Energy Rev.* **2017**, *78*, 780–797. [[CrossRef](#)]
- Duck, B.C.; Fell, C.J. Improving the Spectral Correction Function. In Proceedings of the 43rd IEEE Photovoltaic Specialists Conference (PVSC), Portland, OR, USA, 5–10 June 2016; pp. 2647–2652. [[CrossRef](#)]
- Pierro, M.; Bucci, F.; Cornaro, C. Full Characterization of Photovoltaic Modules in Real Operating Conditions: Theoretical Model, Measurement Method and Results. *Prog. Photovolt. Res. Appl.* **2015**, *23*, 443–461. [[CrossRef](#)]
- Shanks, K.; Senthilarasu, S.; Mallick, T.K. High-Concentration Optics for Photovoltaic Applications. In *High Concentrator Photovoltaics. Fundamentals, Engineering and Power Plants*; Pérez-Higueras, P.J., Fernández, E.F., Eds.; Springer International Publishing: Geneva, Switzerland, 2015; pp. 85–114. [[CrossRef](#)]
- Fernández, E.F.; Soria-Moya, A.; Almonacid, F.; Aguilera, J. Comparative Assessment of the Spectral Impact on the Energy Yield of High Concentrator and Conventional Photovoltaic Technology. *Sol. Energy Mater. Sol. Cells* **2016**, *147*, 185–197. [[CrossRef](#)]
- Rodrigo, P.M.; Fernández, E.F.; Almonacid, F.M.; Pérez-Higueras, P.J. Quantification of the Spectral Coupling of Atmosphere and Photovoltaic System Performance: Indexes, Methods and Impact on Energy Harvesting. *Sol. Energy Mater. Sol. Cells* **2017**, *163*, 73–90. [[CrossRef](#)]
- IEC 60904-7. *Photovoltaic Devices—Part 7: Computation of the Spectral Mismatch Correction for Measurements of Photovoltaic Devices*; International Electrotechnical Commission (IEC): Geneva, Switzerland, 2008.
- Betts, T.R.; Infield, D.G.; Gottschalg, R. Spectral Irradiance Correction for PV System Yield Calculations. In Proceedings of the 19th European Photovoltaic Solar Energy Conference, Paris, France, 7–11 June 2004; pp. 2533–2536.
- Hofmann, M.; Vanicek, P.; Haselbuhn, R. Is the Average Photon Energy (APE) a Suitable Measure to Describe the Uniqueness of Solar Spectra? In Proceedings of the 29th European Photovoltaic Solar Energy Conference and Exhibition, Paris, France, 22–26 September 2014; pp. 3461–3466.
- Dirnberger, D.; Blackburn, G.; Müller, B.; Reise, C. On the Impact of Solar Spectral Irradiance on the Yield of Different PV Technologies. *Sol. Energy Mater. Sol. Cells* **2015**, *132*, 431–442. [[CrossRef](#)]
- Peharz, G.; Siefer, G.; Bett, A.W. A Simple Method for Quantifying Spectral Impacts on Multi-Junction Solar Cells. *Sol. Energy* **2009**, *83*, 1588–1598. [[CrossRef](#)]
- Fernández, E.F.; Almonacid, F. Spectrally Corrected Direct Normal Irradiance Based on Artificial Neural Networks for High Concentrator Photovoltaic Applications. *Energy* **2014**, *74*, 941–949. [[CrossRef](#)]

15. Sutterlueti, J.; Ransome, S.; Kravets, R.; Schreier, L. Characterising PV Modules under Outdoor Conditions: What's Most Important for Energy Yield. In Proceedings of the 26th European Photovoltaic Solar Energy Conference and Exhibition, Hamburg, Germany, 5–11 September 2011.
16. Jardine, C.N.; Betts, T.R.; Gottschalg, R.; Infield, D.G.; Lane, K. Influence of Spectral Effects on the Performance of Multi-junction Amorphous. In Proceedings of the Photovoltaic in Europe—From PV Technology to Energy Solutions, Rome, Italy, 7–11 October 2002.
17. Louwen, A.; de Waal, A.C.; van Sark, W.G. Evaluation of Different Indicators for Representing Solar Spectral Variation. In Proceedings of the 43rd IEEE Photovoltaic Specialists Conference (PVSC), Portland, OR, USA, 5–10 June 2016; pp. 133–137. [[CrossRef](#)]
18. Paudyal, B.R.; Imenes, A.G. Analysis of Spectral Irradiance Distribution for PV Applications at High Latitude. In Proceedings of the 47th IEEE Photovoltaic Specialists Conference (PVSC), Calgary, OR, Canada, 15 June–21 August 2020; pp. 1834–1841. [[CrossRef](#)]
19. Minemoto, T.; Nakada, Y.; Takahashi, H.; Takakura, H. Uniqueness Verification of Solar Spectrum Index of Average Photon Energy for Evaluating Outdoor Performance of Photovoltaic Modules. *Sol. Energy* **2009**, *83*, 1294–1299. [[CrossRef](#)]
20. IEC 60904-9. *Photovoltaic Devices—Part 9: Solar Simulator Performance Requirements*; International Electrotechnical Commission (IEC): Geneva, Switzerland, 2007.
21. Gottschalg, R.; Betts, T.R.; Infield, D.G.; Kearney, M.J. Experimental Investigation of Spectral Effects on Amorphous Silicon Solar Cells in Outdoor Operation. In Proceedings of the Conference Record of the 29th IEEE Photovoltaic Specialists Conference, New Orleans, LA, USA, 19–24 May 2002; pp. 1138–1141. [[CrossRef](#)]
22. Gottschalg, R.; Betts, T.R.; Infield, D.G.; Kearney, M.J. On the Importance of Considering the Incident Spectrum When Measuring the Outdoor Performance of Amorphous Silicon Photovoltaic Devices. *Meas. Sci. Technol.* **2004**, *15*, 460. [[CrossRef](#)]
23. Gottschalg, R.; Betts, T.R.; Infield, D.G.; Kearney, M.J. The Effect of Spectral Variations on the Performance Parameters of Single and Double Junction Amorphous Silicon Solar Cells. *Sol. Energy Mater. Sol. Cells* **2005**, *85*, 415–428. [[CrossRef](#)]
24. Takahashi, H.; Fukushige, S.; Minemoto, T.; Takakura, H. Output Estimation of Si-Based Photovoltaic Modules with Outdoor Environment and Output Map. *J. Cryst. Growth* **2009**, *311*, 749–752. [[CrossRef](#)]
25. Minemoto, T.; Takahashi, H.; Nakada, Y.; Takakura, H. Outdoor Performance Evaluation of Photovoltaic Modules Using Contour Plots. *Curr. Appl. Phys.* **2010**, *10*, S257–S260. [[CrossRef](#)]
26. Nofuentes, G.; de la Casa, J.; Torres-Ramírez, M.; Alonso-Abella, M. Solar Spectral and Module Temperature Influence on the Outdoor Performance of Thin Film PV Modules Deployed on a Sunny Inland Site. *Int. J. Photoenergy* **2013**, *2013*. [[CrossRef](#)]
27. Yoshida, S.; Ueno, S.; Kataoka, N.; Takakura, H.; Minemoto, T. Estimation of Global Tilted Irradiance and Output Energy Using Meteorological Data and Performance of Photovoltaic Modules. *Sol. Energy* **2013**, *93*, 90–99. [[CrossRef](#)]
28. Cornaro, C.; Andreotti, A. Influence of Average Photon Energy Index on Solar Irradiance Characteristics and Outdoor Performance of Photovoltaic Modules. *Prog. Photovolt. Res. Appl.* **2013**, *21*, 996–1003. [[CrossRef](#)]
29. Sirisamphanwong, C.; Sirisamphanwong, C.; Ketjoy, N. The Effect of Average Photon Energy and Module Temperature on Performance of Photovoltaic Module under Thailand's Climate Condition. *Energy Procedia* **2014**, *56*, 359–366. [[CrossRef](#)]
30. Chantana, J.; Imai, Y.; Kawano, Y.; Hishikawa, Y.; Nishioka, K.; Minemoto, T. Impact of Average Photon Energy on Spectral Gain and Loss of Various-Type PV Technologies at Different Locations. *Renew. Energy* **2020**, *145*, 1317–1324. [[CrossRef](#)]
31. Norton, M.; Amillo, A.M.G.; Galleano, R. Comparison of Solar Spectral Irradiance Measurements Using the Average Photon Energy Parameter. *Sol. Energy* **2015**, *120*, 337–344. [[CrossRef](#)]
32. Nofuentes, G.; Gueymard, C.A.; Aguilera, J.; Pérez-Godoy, M.D.; Charte, F. Is the Average Photon Energy a Unique Characteristic of the Spectral Distribution of Global Irradiance? *Sol. Energy* **2017**, *149*, 32–43. [[CrossRef](#)]
33. Tsuji, M.; Rahman, M.M.; Hishikawa, Y.; Nishioka, K.; Minemoto, T. Uniqueness Verification of Solar Spectrum Obtained from Three Sites in Japan Based on Similar Index of Average Photon Energy. *Sol. Energy* **2018**, *173*, 89–96. [[CrossRef](#)]
34. Chantana, J.; Ueno, S.; Ota, Y.; Nishioka, K.; Minemoto, T. Uniqueness Verification of Direct Solar Spectral Index for Estimating Outdoor Performance of Concentrator Photovoltaic Systems. *Renew. Energy* **2015**, *75*, 762–766. [[CrossRef](#)]
35. Gueymard, C.A. Daily Spectral Effects on Concentrating PV Solar Cells as Affected by Realistic Aerosol Optical Depth and Other Atmospheric Conditions. In Proceedings of the SPIE Optical Modeling and Measurements for Solar Energy Systems III, San Diego, CA, USA, 2–4 August 2009. [[CrossRef](#)]
36. Gueymard, C.A. The SMARTS Spectral Irradiance Model after 25 Years: New Developments and Validation of Reference Spectra. *Sol. Energy* **2019**, *187*, 233–253. [[CrossRef](#)]
37. Alonso-Abella, M.; Chenlo, F.; Nofuentes, G.; Torres-Ramírez, M. Analysis of Spectral Effects on the Energy Yield of Different PV (Photovoltaic) Technologies: The Case of Four Specific Sites. *Energy* **2014**, *67*, 435–443. [[CrossRef](#)]
38. García-Domingo, B.; Aguilera, J.; de la Casa, J.; Fuentes, M. Modelling the Influence of Atmospheric Conditions on the Outdoor Real Performance of a CPV (Concentrated Photovoltaic) Module. *Energy* **2014**, *70*, 239–250. [[CrossRef](#)]
39. García, R.; Torres-Ramírez, M.; Muñoz-Cerón, E.; de la Casa, J.; Aguilera, J. Spectral Characterization of the Solar Resource of a Sunny Inland Site for Flat Plate and Concentrating PV Systems. *Renew. Energy* **2017**, *101*, 1169–1179. [[CrossRef](#)]
40. Nofuentes, G.; García-Domingo, B.; Muñoz, J.V.; Chenlo, F. Analysis of the Dependence of the Spectral Factor of Some PV Technologies on the Solar Spectrum Distribution. *Appl. Energy* **2014**, *113*, 302–309. [[CrossRef](#)]

41. Ye, J.Y.; Reindl, T.; Aberle, A.G.; Walsh, T.M. Effect of Solar Spectrum on the Performance of Various Thin-Film PV Module Technologies in Tropical Singapore. *IEEE J. Photovolt.* **2014**, *4*, 1268–1274. [[CrossRef](#)]
42. Nofuentes, G.; de la Casa, J.; Solís-Alemán, E.M.; Fernández, E.F. Spectral Impact on PV Performance in Mid-Latitude Sunny Inland Sites: Experimental vs. Modelled Results. *Energy* **2017**, *141*, 1857–1868. [[CrossRef](#)]
43. Neves, G.; Vilela, W.; Pereira, E.; Yamasoe, M.; Nofuentes, G. Spectral Impact on PV in Low-Latitude Sites: The Case of Southeastern Brazil. *Renew. Energy* **2021**, *164*, 1306–1319. [[CrossRef](#)]
44. Polo, J.; Alonso-Abella, M.; Ruiz-Arias, J.A.; Balenzategui, J.L. Worldwide Analysis of Spectral Factors for Seven Photovoltaic Technologies. *Sol. Energy* **2017**, *142*, 194–203. [[CrossRef](#)]
45. Gueymard, C.A.; Myers, D.; Emery, K. Proposed Reference Irradiance Spectra for Solar Energy Systems Testing. *Sol. Energy* **2002**, *73*, 443–467. [[CrossRef](#)]
46. Gueymard, C.A. Interdisciplinary Applications of a Versatile Spectral Solar Irradiance Model: A Review. *Energy* **2005**, *30*, 1551–1576. [[CrossRef](#)]
47. Myers, D.R. Estimates of Uncertainty for Measured Spectra in the SERI Spectral Solar Radiation Data Base. *Sol. Energy* **1989**, *43*, 347–353. [[CrossRef](#)]
48. Schubert, F.; Klameth, K.; Darou, S.; Spinner, D. Measurement Uncertainties of a Compact Array Spectrometer. *Energy Procedia* **2015**, *77*, 179–186. [[CrossRef](#)]